Possible mechanism in dry micro-electro-discharge machining of carbon-nanotube forests: A study of the effect of oxygen

Masoud Dahmardeh, Alireza Nojeh,[a] and Kenichi Takahata[a]
Department of Electrical and Computer Engineering, The University of British Columbia, Vancouver BC, V6T 1Z4, Canada

(Received 9 February 2011; accepted 2 April 2011; published online 13 May 2011)

The working principle of dry micro-electro-discharge machining of vertically aligned carbon-nanotube forests is investigated by evaluating the effect of oxygen on the process. The machining experiments with controlled oxygen/nitrogen ratios indicate a correlation between the peak current of discharge pulses and the oxygen concentration, suggesting not only a vital role for oxygen in the process, but also a removal mechanism fundamentally different from that in typical electro-discharge machining based on direct melting and evaporation of the sample material. The highest surface quality and uniformity in the machined forest microstructures as well as smooth machining without short circuiting are achieved at an approximate oxygen concentration of 20% under the discharge condition of 30 V and 10 pF, revealing that air is an optimal medium for the removal process. Elemental and molecular analyses show no evidence of significant crystalline deterioration or contamination in the nanotubes processed with the technique. © *2011 American Institute of Physics*. [doi:10.1063/1.3587158]

I. INTRODUCTION

Vertically aligned carbon nanotubes, so called CNT forests, have attracted extensive interest due to their unique electrical, mechanical, thermal, and other properties.[1–3] This material provides a broad range of application opportunities, including field emitters,[4] chip-cooling heat sinks,[5] supercapacitors,[6] biomimetic dry adhesives,[7] and micro-electro-mechanical systems (MEMS).[8] To design and fabricate devices based on CNT forests, there is a fundamental need to define the dimensions of the forests precisely. Lithographic techniques were reported for patterning of disordered CNT layers.[9,10] For patterning of aligned CNT forests, selective chemical vapor deposition (CVD) of the material on predefined catalyst patterns has been widely used.[11–13] The shapes of the grown forests are, however, primarily limited to 2-dimensional-like structures with a uniform height. To facilitate the application of this material to MEMS and other disciplines, it is essential to establish techniques to create 3-dimensional (3-D) free-form microstructures from pregrown forests. Micro-electro-discharge machining (μEDM) of carbon nanofibers[14,15] as well as DC arc discharge machining of CNT forests[16] have been reported for surface patterning of the materials with low aspect ratios. A pulsed μEDM process for 3-D, high-aspect-ratio micromachining of pure CNT forests has recently been developed by the authors[17,18]; this technique has been shown to be highly effective in forming arbitrary micro-scale geometries in the forests, as demonstrated in the produced sample structures shown in Fig. 1. μEDM utilizes pulses of thermomechanical impact induced by a miniaturized electrical discharge generated between a microscopic electrode and a workpiece that can essentially be any electrically conductive material.[19] The miniaturized arc discharge locally melts and evaporates the material at the arc spot, and micromachining is performed by repeating the unit removal by a single pulse at high frequencies while controlling the relative position between the electrode and the workpiece. The typical μEDM process for bulk materials is conducted in a dielectric liquid (such as oil or de-ionized water). On the other hand, to the best of the authors' knowledge, all the μEDM processes of pure CNTs have been performed in dry ambient, specifically in air, mainly in order to avoid the collapse of the forest structures due to the capillary force resulted when the wetted structures are dried (regular μEDM in oil for CNT-polymer composites has been reported in Wan *et al.*[20]). However, the effects of the ambient gas in the dry μEDM for CNT-forest micromachining have not been studied. Kunieda *et al.* showed that the efficiency of macro-scale dry EDM for metal machining could be improved by supplying oxygen to the ambient.[21] In the present paper, the effect of oxygen in CNT-forest μEDM is investigated, revealing a strong dependence of the process on the oxygen concentration in the ambient of nitrogen.

II. SAMPLE PREPARATION AND EXPERIMENTAL SET-UP

The CNT forest samples used in this study were grown on silicon substrates with iron catalyst through an ethylene-based CVD process at 750° C; the catalyst-substrate preparation and the CVD process followed the same conditions reported in Khalid *et al.*[17] Forests of vertically aligned multi-walled CNTs (MWNTs) with lengths of up to several 100 μm were obtained. μEDM experiments were carried out with a 3-axis μEDM machine (EM203, SmalTec International, USA) that employed relaxation-type resistor-capacitor (*R-C*) circuitry for pulse generation/timing.[22] As opposed to the DC arc technique,[16] this μEDM process, which uses nanosecond pulses of arc discharge for machining, potentially enables precise control of discharge energy delivered to a CNT forest while protecting the sample from overheating.[23]

[a]Authors to whom correspondence should be addressed. Electronic addresses: anojeh@ece.ubc.ca and takahata@ece.ubc.ca.

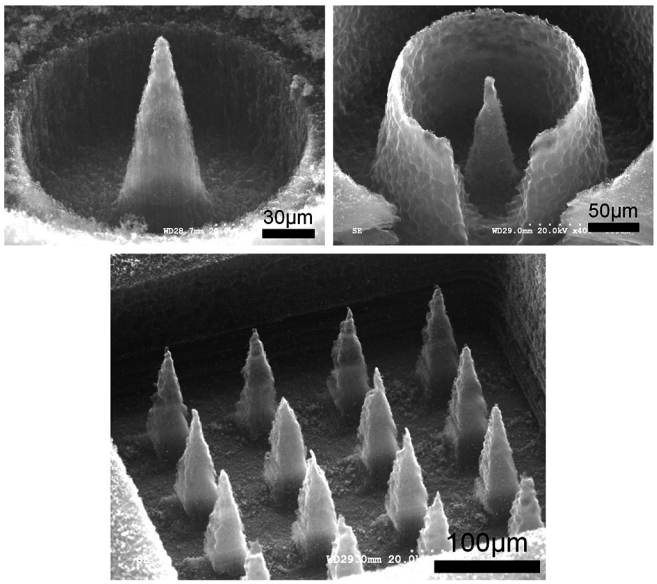

FIG. 1. Needlelike structures with controlled sidewall angles created by dry μEDM[18] © 2011 IEEE.

The experimental set-up used for dry μEDM characterization is shown in Fig. 2. Oxygen is first mixed with nitrogen, an inert dilute gas, inside a buffer chamber, and the mixed gas is introduced to the machining chamber, where the O_2 concentration is measured using an oxygen sensor (VN202, Vandagraph Co., UK). The flow rates of O_2 and N_2 are adjusted so that the O_2 concentration reaches the target value and is stabilized in the machining chamber for at least 10 mins prior to machining. In this study, the O_2 concentrations of 0% (oxygen free), 6%, 10%, 21% (approximately equal to the ratio in air), and 50% were tested. A tungsten electrode (32–100 μm diameter) and the CNT forest are connected as the cathode and the anode, respectively, with the *R-C* circuit as shown in Fig. 2. The electrode feed rate in the vertical (Z) direction was set to be 0.5 μm/s. The μEDM machine has a feedback control system such that when a short circuit between the electrode and the sample (which prevents the discharge generation, i.e., material removal) is detected, the system retracts the electrode up while checking the status of the short circuit and resumes machining by feeding the electrode as soon as the circuit is opened. The machining experiments were conducted with an optimal condition (machining

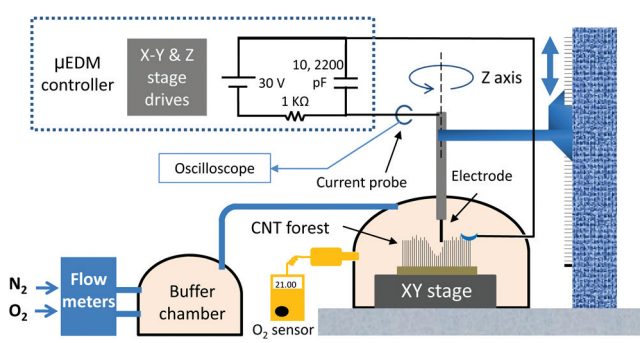

FIG. 2. (Color online) Experimental set-up for dry μEDM of CNT forests with controlled oxygen concentrations in O_2/N_2 ambient.

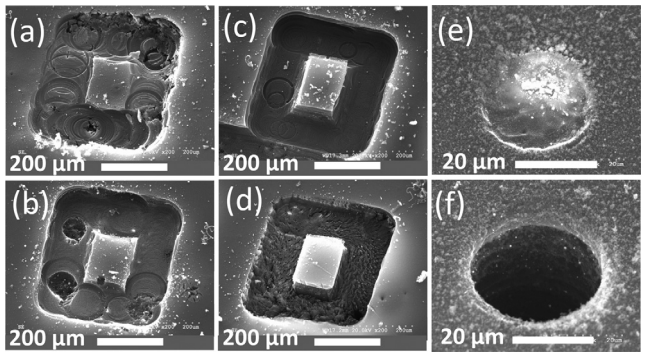

FIG. 3. SEM images of μEDMed CNT forests in N_2 gas mixed with (a) 0% O_2 (oxygen free), (b) 10% O_2, (c) 21% O_2, (d) 50% O_2. Drilling results in (e) pure N_2 and (f) air.

voltage 30 V; capacitance 10 pF; electrode rotation speed 3000 rpm; X–Y feed rates 1 mm/min) that was previously developed for μEDM of CNT forests in air.[17]

III. RESULTS AND DISCUSSION

Figures 3(a)–3(d) show the microstructures machined with different O_2 concentrations and the machining conditions noted above, by scanning a 100-μm-diameter electrode along a rectangular pattern (300 μm × 400 μm) in the X–Y directions while feeding the tool in the Z direction to a depth of 40 μm. The results indicate that the process at 0% O_2 [Fig. 3(a)] resulted in the lowest removal quality, and that the uniformity and the surface smoothness of the machined structures were consistently improved as the O_2 concentration was increased to 21% [Fig. 3(c)]. As can be seen in the drilling results in N_2 [Fig. 3(e)] and in air [Fig. 3(f)] performed under the same EDM conditions, the CNT removal in air is as effective as the 21% O_2 case. Machining in 50% O_2 [Fig. 3(d)], however, led to rougher surfaces compared to those at 21% O_2 as apparent from the SEM images. To visualize the progression of electrode feeding and the impact of oxygen on the feeding, the Z position of the electrode was tracked during drilling of a forest to a depth of 50 μm with different O_2 concentrations [Fig. 4]. The results with the 21% and 50% O_2 concentrations showed smooth feeding with no short-circuit detection, reaching the target depth

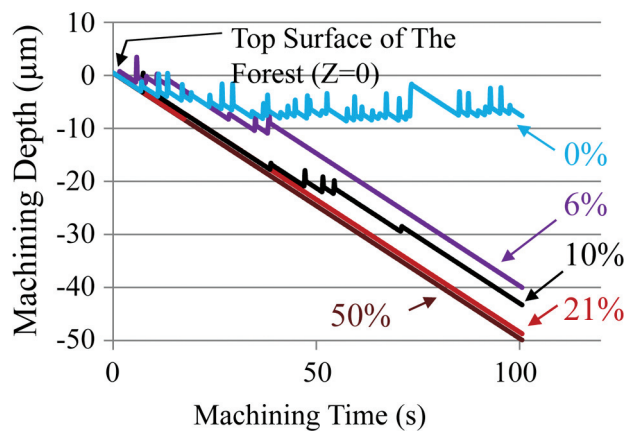

FIG. 4. (Color online) Progressions of electrode feeding in μEDM of a CNT forest with different O_2 concentrations in N_2 at 30 V and 10 pF.

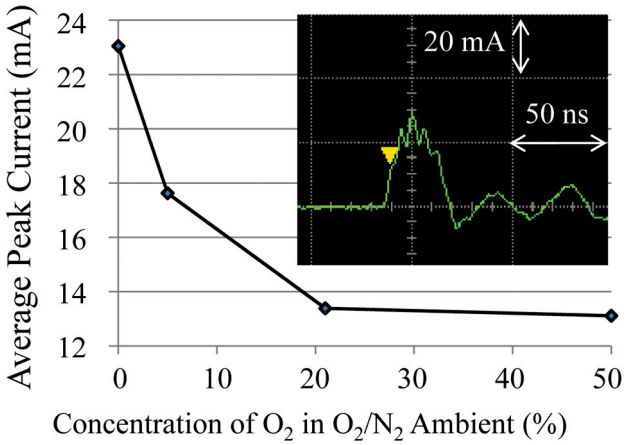

FIG. 5. (Color online) Measured average peak current of discharge pulses as a function of the O_2 concentration at 30 V and 10 pF (the inset shows a typical pulse observed in 21% O_2 at 30 V and 10 pF).

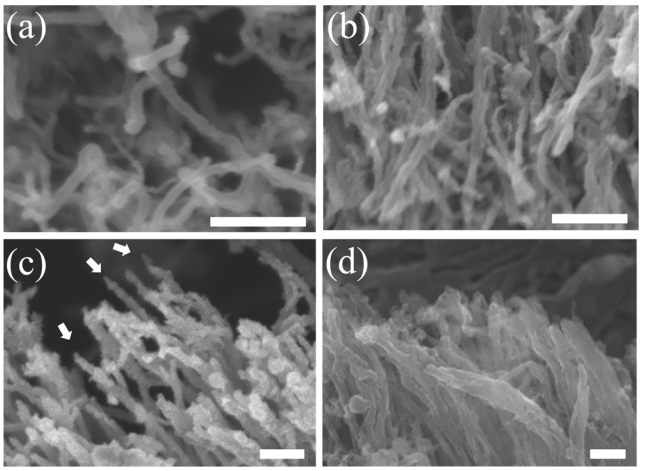

FIG. 6. SEM images of (a) original CNT forest before μEDM, and μEDMed CNT forest (b) in air, and with O_2 concentrations of (c) 0%, and (d) 50% in N_2 (scale bar size in each image is 200 nm).

within the ideal machining time of 100 seconds (i.e., [50 μm]/[0.5 μm/s]). As the concentration was lowered, zigzag patterns appeared, due to the occurrence of short circuits and the resultant controlled retraction of the electrode. It is clearly seen that lowering the O_2 concentration below 21% deteriorates the machining efficiency. For the oxygen-free case, machining beyond 10 μm of depth was not achieved. To probe the EDM dependence on oxygen, the discharge current was measured under identical EDM conditions (30 V, 10 pF) with varying O_2 concentrations using a current probe (CT-1, Tektronix, USA) inserted in the discharge circuit, as shown in Fig. 2. Figure 5 plots the average peak current of discharge pulses ($n = 600$) measured as a function of the O_2 concentration. It can be seen that the average peak current drops as the O_2 concentration increases and saturates ($\sim$13 mA) at around 21% O_2. This saturation is likely related to the results in Fig. 4, which show similar straight feeding paths for the O_2 concentrations of 21% and 50%. The discharge current is the highest ($\sim$23 mA) at 0% O_2, while proper machining at this condition is barely feasible. This condition does not follow the typical relationship between the discharge current and the material removal rate in regular EDM, in which larger discharge currents lead to higher removal rates in general. It has been suggested that the lower current carrying capacity of MWNTs in the presence of oxygen is mainly because of the loss of individual carbon shells due to thermal oxidation.[24,25] This characteristic is consistent with the measured result in Fig. 5, which shows the highest current in the absence of oxygen and little removal of CNTs. Based on the results observed, the removal of CNTs in the μEDM process may be related to the thermally enhanced oxidation, rather than direct melting/evaporation due to heat provided by the discharge pulses as the typical removal mechanism in EDM; in other words, this CNT μEDM may essentially be a pulsed process of local oxygen plasma etching of the nanotubes.

To evaluate the structures of the processed nanotubes, high-resolution scanning electron microscopy (SEM) was performed for the surfaces of the machined structures shown in Fig. 3 and for an unprocessed area near the structures [Figs. 6(a)–6(d)]. For low concentrations of O_2 (up to 21%), some of the CNTs developed sharp tips (indicated by arrows in Fig. 6(c)), resembling the needle-shaped bundles of CNTs after plasma etching reported in Liu *et al.*,[26] while other CNTs exhibited different morphologies with rougher surfaces compared to those of the original CNTs with smooth surfaces (similar results were reported in Yu *et al.*[27]). For 50% O_2, thickening of CNTs is evident; this could be related to the formation of thicker bundles of individual CNTs and/or the adsorption of the carbon debris produced in the machining process.[17] The analysis of the machined samples with energy-dispersive X-ray spectroscopy (EDX) showed no noticeable difference between the results with different O_2 concentrations. Tungsten was not observed in the EDX results, suggesting negligible electrode consumption during the μEDM process under the employed machining conditions. In order to evaluate the impact of μEDM on the crystalline properties of the CNTs, Raman spectra were collected from the μEDMed regions in the structures shown in Figs. 3(a), (c), and (d) machined in the forest with the O_2 concentrations of 0%, 21%, and 50%, respectively, as well as from the original CNTs in the same forest for comparison [Fig. 7]. The G mode that arises from the sp^2 C crystalline structures and the D mode related to crystalline defects[28] are seen in the collected data. As shown in the graph, the I_D/I_G ratios in the original and μEDMed forest surfaces are very close (0.76–0.79), suggesting that the impact of μEDM on the CNT's crystalline properties under the used conditions is minimal. The DC arc discharge machining of CNT forests has been reported to lower the I_D/I_G ratio.[16] It is also known that high-density oxygen plasma treatment of CNTs causes defects in them.[29] The Raman analysis in the present study provided no evidence of significant I_D/I_G ratio reduction or increased defects in the CNTs processed with the pulsed μEDM used. A closer look at Fig. 7 reveals that for the oxygen-free (0%) condition, the G and D peaks are shifted by $\sim$22 and $\sim$12 cm^{-1} from the peaks (at 1570 and 1340 cm^{-1}, respectively) for the nonzero O_2 concentrations to the higher wavenumber side. The shifts were observable in Raman data from some locations on the surfaces

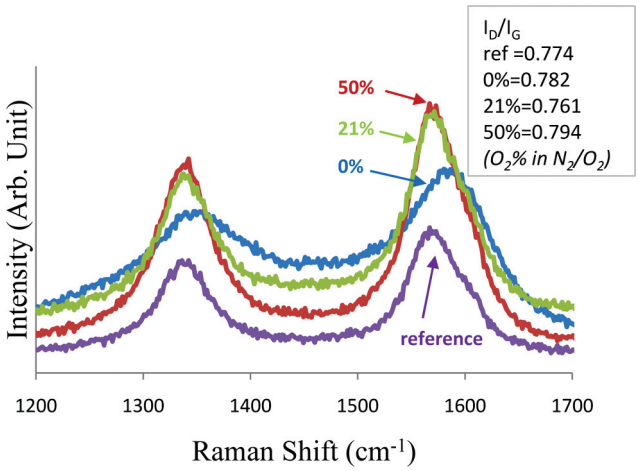

FIG. 7. (Color online) Raman spectra of the CNT forest before and after μEDM with different O_2 concentrations in N_2.

machined under the oxygen-free condition but were not consistent over the entire area of the surfaces. It has been suggested that the compressive thermal strain causes shifts of the G-mode peak.[30–32] In the machining process, uncontrolled spontaneous large sparks were occasionally observed at low concentrations (0–10%) of oxygen; the observed Raman shifts in the oxygen-free case could be related to high current stressing of the carbon nanotubes caused by the large sparks.

IV. CONCLUSIONS

The effect of oxygen in dry μEDM of CNT forests was investigated. The experimental results revealed that oxygen plays a critical role in the removal process, suggesting that localized oxygen plasma etching induced by pulsed arc discharges, unlike the direct thermal removal in regular μEDM, may be the main removal mechanism of the process. It was found that the use of oxygen-free, 100%-nitrogen ambient prevents proper CNT removal. The process at the O_2 concentration of ~21% in nitrogen achieved not only the highest machining quality among all O_2 concentrations tested but also efficient CNT removal, without suffering from short circuiting during the process. This suggests that air may be a suitable, and in fact, optimal medium for dry μEDM of the forests. Thickening of the tips of the processed CNTs was observed, which could be related to the adsorption of the removed carbon atoms and bundling of the CNTs. The Raman and EDX analyses, however, suggest that the μEDM process may not cause significant crystalline deterioration in the CNTs and contamination with the electrode elements.

ACKNOWLEDGMENTS

The authors thank Parham Yaghoobi for his assistance in CNT sample preparation. This work was partially supported by the Natural Sciences and Engineering Research Council of Canada, the Canada Foundation for Innovation, and the British Columbia Knowledge Development Fund.

[1]N. Hamada, S. Sawada, and A. Oshiyama, Phys. Rev. Lett. **68**, 1579 (1992).
[2]J. P. Lu, Phys. Rev. Lett. **79**, 1297 (1997).
[3]M. M. J. Treacy, T. W. Ebbesen, and J. M. Gibson, Nature (London) **381**, 678 (1996).
[4]O. Groning, O. M. Kuttel, C. Emmenegger, P. Groning, and L. Schlapbach, J. Vac. Sci. Technol. B **18**, 665 (2000).
[5]K. Kordas, G. Toth, P. Moilanen, M. Kumpumaki, J. Vahakangas, A. Uusimaki, R. Vajtai, and P. M. Ajayan, Appl. Phys. Lett. **90**, 123105 (2007).
[6]C. Du and N. Pan, Nanotechnology **17**, 5314 (2006).
[7]L. Ge, S. Sethi, L. Ci, P. M. Ajayan, and A. Dhinojwala, Proc. Natl. Acad. Sci. U.S.A. **104**, 10792 (2007).
[8]Y. Hayamizu, T. Yamada, K. Mizuno, R. C. Davis, D. N. Futaba, M. Yumura, and K. Hata, Nature Nanotech. **3**, 289 (2008).
[9]A. Behnam, Y. Choi, L. Noriega, Z. Wu, I. Kravchenko, A. G. Rinzler, and A. Ural, J. Vac. Sci. Technol. B **25**, 348 (2007).
[10]J. Chae, X. Ho, J. A. Rogers, and K. Jain, Appl. Phys. Lett. **92**, 173115 (2008).
[11]A. J. Hart and A. H. Slocum, J. Phys. Chem. B **110**, 8250 (2006).
[12]J. I. Sohn, S. Lee, Y. Song, S. Choi, K. Cho, and K. Nam, Appl. Phys. Lett. **78**, 901 (2001).
[13]K. Hata, D. Futaba, K. Mizuno, T. Namai, M. Yumura, and S. Iijima, Science **306**, 1362 (2004).
[14]J. G. Ok, B. H. Kim, W. Y. Sung, C. N. Chu, and Y. H. Kim, Appl. Phys. Lett. **90**, 033117 (2007).
[15]J. G. Ok, B. H. Kim, D. K. Chung, W. Y. Sung, S. M. Lee, S. W. Lee, W. J. Kim, J. W. Park, C. N. Chu, and Y. H. Kim, J. Micromech. Microeng. **18**, 025007 (2008).
[16]Y. W. Zhu, C. H. Sow, M. C. Sim, G. Sharma, and V. Kripesh, Nanotechnology **18**, 385304 (2007).
[17]W. Khalid, M. S. Mohamed Ali, M. Dahmardeh, Y. Choi, P. Yaghoobi, A. Nojeh, and K. Takahata, Diam. Rel. Mater. **19**, 1405 (2010).
[18]M. Dahmardeh, W. Khalid, M. S. Mohamed Ali, Y. Choi, P. Yaghoobi, A. Nojeh, and K. Takahata, in 24th IEEE International Conference on Micro Electro Mechanical Systems (MEMS), Cancun, Mexico, January 2011, pp. 272–275.
[19]K. Takahata, *Micro Electronic and Mechanical Systems* (InTech, 2009), Chapter 10.
[20]Y. Wan, D. Kim, Y. B. Park, and S. K. Joo, Adv. Compos. Lett. **17**, 115 (2008).
[21]M. Kunieda, S. Furuoya, and N. Taniguchi, Ann. CIRP Ann **40**, 215 (1991).
[22]Y. S. Wong, M. Rahman, H. S. Lim, H. Han, and N. Ravi, J. Mater. Process. Technol. **140**, 303 (2003).
[23]M. Kunieda, B. Lauwers, K. P. Rajurkar, and B. M. Schumacher, CIRP Annals Manufac. Technol. **54**, 64 (2005).
[24]P. G. Collins, M. Hersam, M. Arnold, R. Martel, and Ph. Avouris, Phys. Rev. Lett. **86**, 3128 (2001).
[25]P. M. Ajayan, T. W. Ebbesen, T. Ichihashi, S. Iijima, K. Tanigaki, and H. Hiura, Nature (London) **362**, 522 (1993).
[26]Y. Liu, L. Liu, P. Liu, L. Sheng, and S. Fan, Diam. Rel. Mater. **13**, 1609 (2004).
[27]K. Yu, Z. Zhu, Y. Zhang, Q. Li, W. Wang, L. Luo, X. Yu, H. Ma, Z. Li, and T. Feng, Appl. Surf. Sci. **225**, 380 (2004).
[28]M. S. Dresselhaus, G. Dresselhaus, R. Saito, and A. Jorio, Phys. Rep. **409**, 47 (2004).
[29]C. Juan, C. Tsai, K. Chen, L. Chen, and H. Cheng, Jpn. J. Appl. Phys. **44**, 8231 (2005).
[30]Z. Li, P. Dharap, S. Nagarajaiah, E. V. Barrera, and J. D. Kim, Adv. Mater. **16**, 640 (2004).
[31]J. Sandler, M. Shaffer, A. Windle, M. Halsall, M. Montes-Morán, C. Cooper, and R. Young, Phys. Rev. B **67**, 035417 (2003).
[32]S. Ruan, P. Gao, X. Yang, and T. Yu, Polym. **44**, 5643 (2003).